

## Local bonding geometry of O(2×1) on Ni(110): A surface extended x-ray-absorption fine-structure study

K. Baberschke, U. Döbler, L. Wenzel, and D. Arvanitis

*Institut für Atom- und Festkörperphysik, Freie Universität Berlin, D-1000 Berlin 33, West Germany*

A. Baratoff and K. H. Rieder

*IBM Zurich Research Laboratory, 8803 Rüschlikon, Switzerland*

(Received 17 December 1985)

Oxygen *K*-edge surface extended x-ray-absorption fine-structure spectra measured with significantly improved signal-to-noise ratio reveal novel features of the intriguing (2×1) oxygen-induced reconstruction of Ni(110). The spectrum obtained for *E* parallel to [001] unambiguously indicates that each oxygen sits in a long-bridge position 0.56 Å away from the nearest topmost Ni row. The relatively short Ni-O distance inferred from data obtained with *E* parallel to  $\bar{1}10$  can only be explained if each oxygen is tilted towards (100) facets of the reconstructed substrate. The amplitude ratio  $A^{\bar{1}10}/A^{001}$  favors the sawtooth model over the missing-row model.

The initial step of chemisorption of oxygen on the open (110) surfaces of the fcc metals Ni and Cu is still poorly understood: It is believed that oxygen induces a reconstruction of the substrate. A theoretical grasp of the underlying physics, and a unique experimental proof of this conjecture would be an important step in understanding the relation between chemisorption and oxidation.

Within the past two years, new information has been obtained for O(2×1)/Ni(110) by ion-channeling-induced Auger yields,<sup>1</sup> scanning-tunneling microscopy,<sup>2</sup> He diffraction,<sup>3</sup> alkali-ion impact collision scattering (ALICIS),<sup>4</sup> and spin-polarized photoemission spectroscopy (SPPEs)<sup>5</sup> as well as for the same superstructure of O on Cu(110) from surface extended x-ray-absorption fine-structure (SEXAFS),<sup>6</sup> angle-resolved photoemission spectroscopy (ARPES),<sup>7</sup> ALICIS,<sup>8</sup> and glancing-incidence x-ray diffraction.<sup>9</sup> Here, we present SEXAFS results for O(2×1)/Ni(110). The combination with previous data gives for the first time a more complete, physically reasonable picture of this adsorbate-induced reconstruction in real space: (i) The oxygens occupy tilted long-bridge sites above the first Ni layer, a possibility first suggested on the basis of low-energy ion scattering.<sup>10</sup> (ii) The Ni layers reconstruct according to a sawtooth model.<sup>1</sup> The driving force for this appears to be oxygen bonding, preferring higher coordination as on the (100) surface.

We first describe our O(2×1)/Ni(110) SEXAFS measurements which were obtained with the same crystal as in the scanning-tunneling microscopy (STM) work, using a well established procedure for preparing the O(2×1) structure.<sup>2,3</sup> Then we discuss our SEXAFS results in the light of previous work, and conclude that our data cannot be explained by the missing-row model.

The base pressure in the ultrahigh vacuum chamber was  $2 \times 10^{-10}$  Torr. After an exposure to  $\approx 0.8$  langmuir ( $1 \text{ L} = 10^{-6} \text{ Torr sec}$ ) oxygen at  $T = 190^\circ \text{C}$ , the LEED pattern indicated a sharp 2×1 superstructure. According to Ref. 2 and previous studies,<sup>11</sup> the effective coverage corresponds to  $\approx \frac{1}{3}$  monolayer. SEXAFS measurements were performed at the storage ring Berliner Elektronenspeicherring-Gesellschaft für Synchrotronstrahlung (BESSY) with

the SX-700 monochromator using a 1200 lines/mm grating. Most of the experimental details were as described in Ref. 6. However, the recent improvement of the storage ring provided a more intense ( $< 750 \text{ mA}$ ) and more stable beam. Figure 1 shows our SEXAFS spectrum for normal incidence and the electric field vector *E* parallel to [001]. Comparison with Fig. 1 of Ref. 6 shows the improved signal-to-noise ratio. To our knowledge, this spectrum has the best statistics ever published in submonolayer SEXAFS, and demonstrates the potential for further work on low-*Z* adsorbate overlayers. Because of the Ni *L* edge, data were taken only up to 820 eV photon energy.

Figure 1 shows a jump of  $\approx 6\%$  at the O *K* absorption edge in agreement with the O/Cu(110) data.<sup>6</sup> The Fourier transform (FT) of the SEXAFS oscillations clearly yields two peaks *A* and *B*. Because the noise in the FT is so small, peak *B* can be unambiguously associated with a second backscatterer. Peak *A* can safely be attributed to the Ni nearest neighbors. Using the scattering phase shift  $\Phi_s = 7.7 - 0.75 \text{ Å} \times k$  from bulk NiO,<sup>12</sup> one calculates a nearest-

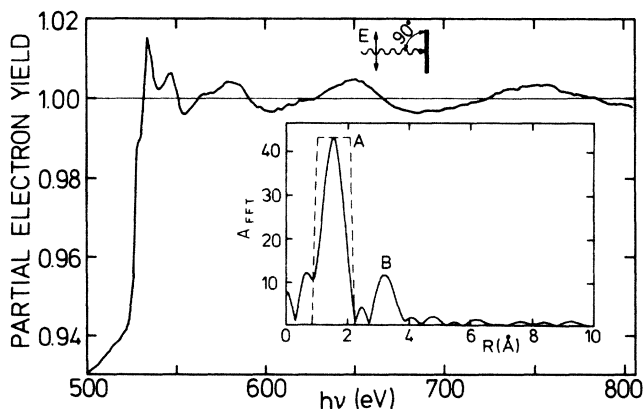


FIG. 1. Partial electron yield (using 350 eV retarding voltage) after background subtraction. The *E* vector lies parallel to [001]. The dashed line in the Fourier transform (inset) indicates the window for the back transformation in Fig. 2.

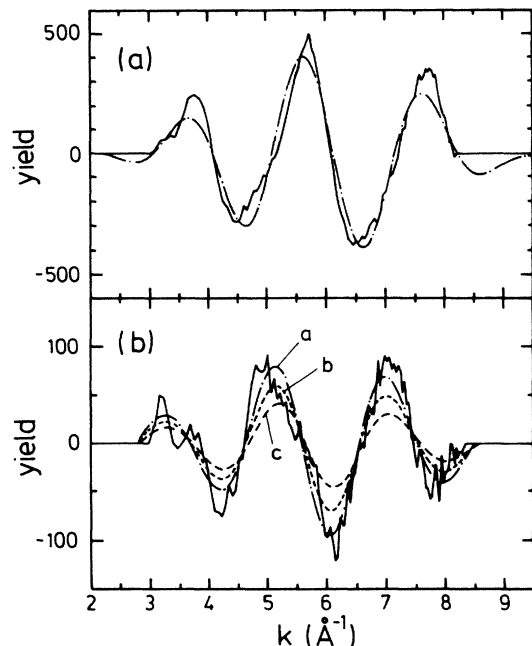


FIG. 2. Experimental spectra and fits for E parallel (a) [001] and (b)  $[\bar{1}10]$ . The parameters for the three fits (a,b,c) in (b) are given in Table I and in the text.

neighbor distance in the [001] direction of  $R_1^{001} = 1.85 \text{ \AA}$ . The interpretation of peak B is more difficult, since *a priori* one does not know whether the corresponding backscatterer is O or Ni.

In the spectrum measured with E parallel to  $[\bar{1}10]$ , the SEXAFS amplitude is reduced roughly by a factor of 5 (Fig. 2) and the distance to the nearest backscatterer is only slightly larger,  $R_1^{\bar{1}10} = 1.96 \text{ \AA}$ . The three parameters  $R_1^{001}$ ,  $R_1^{\bar{1}10}$ , and the amplitude ratio for normal incidence  $A^{\bar{1}10}/A^{001} = 0.19$  are the most reliable ones, and form the basis of our analysis. We also measured SEXAFS spectra for  $\theta = 45^\circ$  and  $20^\circ$  with E in the (001) plane, but these data have larger error bars and are less reliable. The experimental results are summarized in Table I, where distances were determined in the frame of single-scattering theory and phase-shift transferability,<sup>13</sup> and all other systematic errors have been included.

Before analyzing our data, we briefly review the most current model structures. The clean unreconstructed surface shows channels parallel to  $[\bar{1}10]$ . The corresponding  $1 \times 1$  LEED pattern changes into a  $2 \times 1$  upon exposure to oxygen with unit periodicity parallel to [001]. Ion scatter-

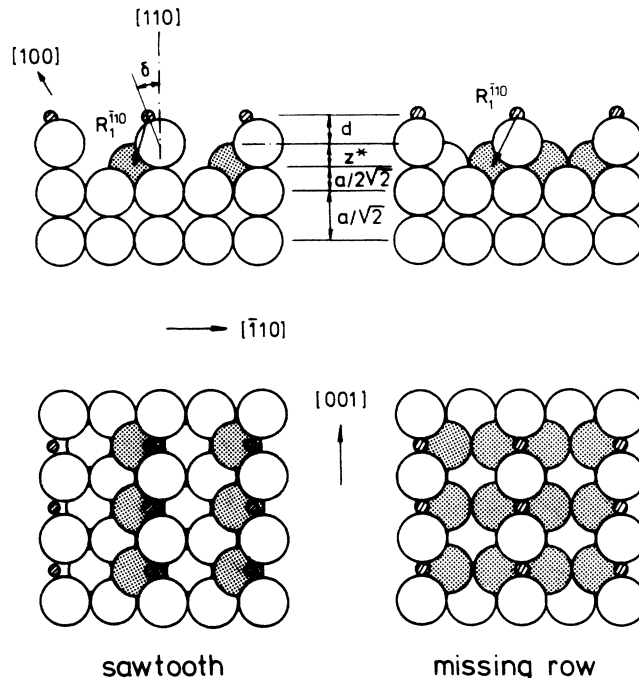


FIG. 3. Two model structures for Ni(110): For zero vertical relaxation  $z^* = a/2^{3/2}$ ;  $d$  is the vertical height above the first layer of Ni atoms. For small tilt angles  $\delta$ , the value of  $d$  is slightly reduced (see Fig. 4 and text).

ing<sup>4,10</sup> and channeling,<sup>1,11</sup> as well as He scattering<sup>3</sup> and SPPEs<sup>5</sup> indicated that the substrate is reconstructed, with only small displacements in the two topmost Ni layers, however.<sup>11</sup> This is consistent with both the sawtooth model<sup>1,6</sup> sketched in Fig. 3, and the missing-row model of Fig. 3.<sup>4,10</sup> The real-space image provided by STM<sup>2</sup> furthermore suggests that the surface exhibits domains of average length of  $60a$  parallel to [001] and only several periods along  $[\bar{1}10]$ . For such chemically induced substrate reconstructions, one should, in principle, allow vertical relaxation between the layers, horizontal relaxation (row pairing), and a tilt angle  $\delta$  for the adsorbate. In previous investigations attempting to distinguish between the above-mentioned models,<sup>1,3,4</sup> these refinements have not been considered.

Our SEXAFS analysis can clarify only the nearest-neighbor environment; the determination of third nearest neighbors is already difficult. This has an important implication, as can be seen from Fig. 4: If oxygen is in the position indicated, it is easy to measure the SEXAFS oscillations

TABLE I. Experimental values for  $R$ , amplitude ratios, and calculated amplitude values for different models and orientations. SI and MR denote sawtooth and missing-row models, respectively.

Orientation	$\theta$	Expt. $R$ ( $\text{\AA}$ )	Expt. amplitude ratio	Calc. amplitude ratio					
				(a) $\delta = 0^\circ$ relax: 23%		(b) $\delta = 20^\circ$ relax: 10%		(c) $\delta = 33^\circ$ relax: 0%	
				ST	MR	ST	MR	ST	MR
[001]	$90^\circ$	1.85(3)	1	1	1	1	1	1	1
[001]	$45^\circ$	1.87(8)	0.48(10)	0.69	0.83	0.72	0.82	0.73	0.81
[001]	$20^\circ$	1.88(10)	0.37(15)	0.47	0.71	0.51	0.68	0.52	0.67
$[\bar{1}10]$	$90^\circ$	1.96(8)	0.19(9)	0.19	0.38	0.16	0.30	0.14	0.27

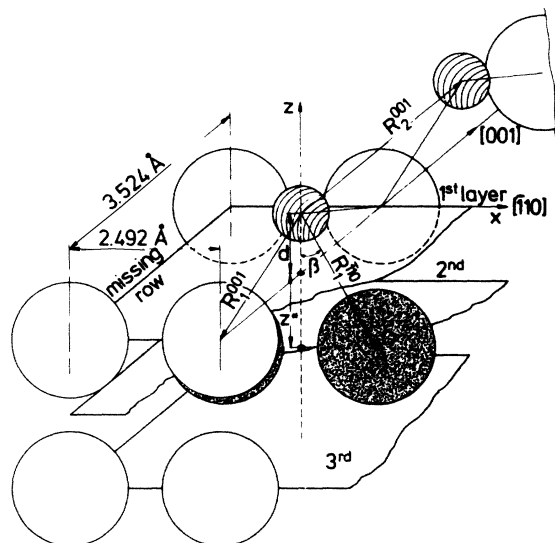


FIG. 4. Schematic geometry of the chemisorption site for zero tilt. Ni atoms (large spheres) in rows adjacent to rows with O atoms (hatched sphere) in long-bridge sites are missing in both models, but one of the Ni atoms in the second layer (shaded spheres) is absent in the sawtooth model.

associated with nearest neighbors in (001) and in  $(\bar{1}10)$  planes, but impossible to decide directly whether the adjacent Ni row in the top layer is occupied, i.e., to distinguish between weak (e.g., buckling) and strong substrate reconstructions. We interpret our data in the following steps.

(i) The fact that one finds different oscillation periods and amplitudes for  $\mathbf{E}$  parallel to [001] and  $[\bar{1}10]$ , and that  $R_{\bar{1}10}^{001} < R_{\bar{1}10}^{\bar{1}10}$  unambiguously leads<sup>6,13</sup> to a long-bridge adsorption site with the adatom above the first Ni layer. It is impossible for oxygen to sit between the first and second layers without causing an unphysically large expansion that is excluded by ion channeling and blocking measurements.<sup>11</sup>

(ii) All groups report sharp LEED spots with unit periodicity along [001]; thus it is commonly accepted that in the [001] rows of the top layer, the Ni atoms retain their bulk spacing, i.e., the lattice constant  $a = 3.52 \text{ \AA}$ . Using  $R_{\bar{1}10}^{001} = 1.85 \text{ \AA}$ , we calculate a distance  $d = 0.56(9) \text{ \AA}$  for the oxygen from the topmost Ni row independent of any tilt angle  $\delta$  with respect to the surface normal.  $2R_{\bar{1}10}^{001}$  is slightly larger than  $a$ , yielding an out-of-plane angle  $\pi/2 - \beta^{100}$  of  $\approx 17.7^\circ$ .

(iii) We now determine a reasonable nearest-neighbor geometry in the perpendicular plane consistent with two crucial experimental facts, namely, that  $R^{\bar{1}10}$  is only 0.11 Å longer than  $R_{\bar{1}10}^{001}$  and that the amplitude is reduced by a factor of  $\approx 5$ . For  $\text{O}(2 \times 1)/\text{Cu}(110)$ ,<sup>6</sup> the difference in radii and the amplitude ratio were larger. The amplitude depends on the nearest-neighbor distance as<sup>13</sup>  $f(R) \propto R^{-2} \exp(-2R/\lambda)$ . For a reasonable inelastic mean free path  $\lambda \approx 5 \text{ \AA}$ ,  $A^{\bar{1}10}$  would only be reduced by a factor of 0.85 with respect to  $A^{001}$ . Furthermore, the amplitude depends on the projection of the internuclear axes on the  $\mathbf{E}$  vector giving rise to a  $\cos^2 \alpha$  dependence. From Table I, we take  $A^{\bar{1}10}/A^{001} = 0.19$  and calculate  $\alpha^{\bar{1}10} = \pi/2 - \beta^{\bar{1}10}$  (see Fig. 4) using  $A_i = N_i f(R_i) \cos^2 \alpha_i$ ,  $N_i$  being the number of backscatters in one shell.<sup>13</sup> Along [001],  $N_i = 2$ , but for  $[\bar{1}10]$ ,  $N_i = 2$  for the missing row, and  $N_i = 1$  for the sawtooth model. In other words, for the latter model, the

amplitude ratio is already reduced by 50% because there is only one backscatterer (one black sphere in Fig. 4 is missing). This remains true even if the incident beam illuminates several inequivalent domains. The unperturbed lateral distance of the second-layer Ni atoms from their midpoint is  $a/2^{3/2} = 1.246 \text{ \AA}$ . Applying Eq. (2) to the sawtooth model without tilt, one obtains  $\alpha^{\bar{1}10} = 50.5^\circ$  and  $\chi^{\bar{1}10} = R^{\bar{1}10} \cos(\alpha^{\bar{1}10}) = 1.246 \text{ \AA}$  in agreement with the unperturbed lateral position of the second-layer Ni atom. The same calculation for  $N_i = 2$  (missing-row model) yields  $\chi^{\bar{1}10} = 0.881 \text{ \AA}$  implying that the two neighbors of each O (Fig. 4) would be displaced as much as  $\approx 28\%$  towards their midpoint, a very unphysical result. In summary, the strong reduction in the experimental amplitude along  $[\bar{1}10]$  can only be explained with one backscatterer, thus excluding the missing-row model.

(iv) We next calculate the vertical distance (still assuming  $\delta = 0$ )  $R^{\bar{1}10} \sin(50.5^\circ) = 1.535 \text{ \AA}$ . This would correspond to an inwards relaxation between the first and second layers of 23% [see curve a in Fig. 2(b)].

(v) So far, we have allowed vertical and horizontal relaxations, but no finite tilt. From (iii), it is clear that only tilt angles towards the (100) facet are of interest, since the strong reduction of  $A^{\bar{1}10}$  has to be explained. We have considered several combinations of relaxations and tilt angles  $\delta$ . Three are given in Table I:  $\delta = 0$  and 23% relaxation has already been discussed. In the opposite case of no vertical relaxation, one would require  $\delta = 33^\circ$ . For this geometry, curve c in Fig. 2(b) gives a smaller amplitude. Curve b with  $\delta = 20^\circ$  and a 10% relaxation gives a relative amplitude of 0.15 that is within the experimental error bars.

(vi) Finally, we consider the polar angular dependence  $\theta$  of our SEXAFS data (rows 2 and 3 in Table I). These data are less reliable as reflected in the indicated error bars. Nevertheless, a comparison between the calculated amplitudes for the missing-row model and the sawtooth model show that the latter fits better.

(vii) We have already indicated that the excellent statistics allows the determination of a second significant peak  $B$  in the FT for  $\theta = 0$  and  $\mathbf{E}$  parallel to [001] (see Fig. 1). From Fig. 4 and (ii), we know that the O-Ni axis makes an angle of only  $\approx 18^\circ$  with the O-O axis. For such small angles, it is known that the single-scattering approximation is not valid.<sup>14</sup> Hence, we did not use peak  $B$  in our analysis.

The present SEXAFS experiment clearly shows that the oxygen adatoms sit in long-bridge sites above the first Ni layer. The distance  $d$  from the underlying Ni row is  $d = 0.56 \text{ \AA}$ . This value is somewhat larger than claimed in the literature,<sup>1,3,4</sup> but because determined by SEXAFS is a direct measure, and relies only on assumption (ii). To determine  $d$  from He scattering via a fit to the corrugation function based on superposed atomic or ionic charge densities, one has to know the charge transfer to each oxygen. Engel, Rieder, and Batra<sup>3</sup> obtained  $d \approx 0.3$  for  $\text{O}^-$  and  $d \approx 0.7 \text{ \AA}$  for  $\text{O}^0$ . Recent theoretical calculations for  $(2 \times 2)\text{O}/\text{Ni}(100)$  yield a charge transfer which is model dependent, but smaller than  $-1$ , namely,  $\approx -0.2$  (Ref. 15) and  $\approx -0.8$  (Ref. 16). The ALICIS experiments<sup>4</sup> are primarily sensitive to the Ni nuclei so that  $d > 0.3 \text{ \AA}$  may be possible.<sup>17</sup>

The present SEXAFS work strongly supports the sawtooth model. The only recent work which presently disagrees with this is Ref. 4. In the ALICIS patterns, three peaks expected for the sawtooth model are weak or absent, and one attri-

buted to nonreconstructed rows that do not exist in that model, is present. However, the absence of another peak expected from nonreconstructed areas contradicts accumulated evidence for a saturation coverage  $\approx \frac{1}{3}$  ML for the (2×1) structure, including direct observation of such areas by STM.<sup>2</sup> Their presence could account for the ALICIS  $[\bar{1}10]$  peak attributed to nonreconstructed rows. Finally, no tilt angle and no relaxation have so far been allowed in the corresponding simulation.

Another indirect argument in favor of the sawtooth model with a finite tilt is the following. The reconstruction of the substrate is induced by O chemisorption, although the corresponding bonding is local and primarily involves nearest-neighbor Ni atoms. We do not see why the local environment should remain unchanged in such a process. For adsorption in long-bridge sites on the unreconstructed Ni(110) surface and for the missing-row model, the coordination number (2) and the local symmetry of each O would remain the same (see Fig. 4). However, for a finite tilt and a compatible sawtooth deformation of the substrate, both are changed. The tilt is such that O adatoms are displaced towards what would be the favored fourfold hollow sites on the (100) face,<sup>12</sup> but the corresponding facet is truncated and only three Ni neighbors are available. A more quantita-

tive interpretation of the bonding and resulting structure must also account for the activation energy required for the Ni(110) substrate reconstruction.<sup>18</sup>

Finally, we briefly consider the O(2×1)/Cu(110) surface. Rather indirect arguments for a weak reconstruction, e.g., the buckling model proposed on the basis of high-energy ion backscattering,<sup>19</sup> were produced from recent measurements.<sup>7,9</sup> A strong reconstruction is indicated by He scattering<sup>20</sup> and ALICIS,<sup>8</sup> however. The SEXAFS data<sup>6</sup> could be fitted without any tilt or relaxation, and are thus consistent with the missing-row model which is again favored by ALICIS. Note that the amplitude ratio  $A(\bar{1}10)/A(001) = 0.22$  (Table I of Ref. 6) lies between the predictions of the missing-row (0.31) and sawtooth (0.15) models (assuming no tilt).

We thank C. R. Brundle, J. Behm, N. Garcia, H. Niehus, J. R. Pendry, J. Stöhr, and D. Vvedensky for enlightening discussions and K. H. Bennemann for copies of his work prior to publication. Ch. Gerber is acknowledged for putting the Ni crystal at our disposal. The work is supported by Bundesminister für Forschung und Technologie under Grant No. 05 233 BB.

<sup>1</sup>M. Schuster and C. Varelas, *Surf. Sci.* **134**, 195 (1983).

<sup>2</sup>A. M. Baro, G. Binnig, H. Rohrer, Ch. Gerber, E. Stoll, A. Barattoff, and F. Salvan, *Phys. Rev. Lett.* **52**, 1304 (1984).

<sup>3</sup>T. Engel, K. H. Rieder, and I. P. Batra, *Surf. Sci.* **148**, 321 (1984).

<sup>4</sup>H. Niehus and G. Comsa, *Surf. Sci.* **151**, L171 (1985).

<sup>5</sup>R. Claiberg and R. Feder, in *Polarized Electrons in Surface Physics*, edited by R. Feder, *Advanced Series in Surface Science*, Vol. 1 (World Scientific, Singapore, 1985).

<sup>6</sup>U. Döbler, K. Baberschke, J. Haase, and A. Puschmann, *Phys. Rev. Lett.* **52**, 1437 (1984).

<sup>7</sup>R. A. DiDio, D. M. Zehner, and D. W. Plummer, *J. Vac. Sci. Technol. A* **2**, 852 (1984).

<sup>8</sup>H. Niehus and G. Comsa, *Surf. Sci.* **140**, 18 (1984).

<sup>9</sup>K. S. Liang, P. H. Fuoss, G. J. Hughes, and P. Eisenberger, in *The Structure of Surfaces*, edited by M. A. van Hove and S. Y. Tong, *Springer Series in Surface Sciences*, Vol. 2 (Springer, Berlin, 1985), p. 246.

<sup>10</sup>K. K. Verheij, J. A. van den Berg, and D. G. Armour, *Surf. Sci.*

**84**, 408 (1979).

<sup>11</sup>R. G. Smeenk, R. M. Tromp, and F. W. Saris, *Surf. Sci.* **107**, 429 (1981).

<sup>12</sup>J. Stöhr, R. Jaeger, and T. Kendelewicz, *Phys. Rev. Lett.* **49**, 142 (1982).

<sup>13</sup>J. Stöhr, in *Chemistry and Physics of Solid Surfaces V*, edited by R. Vanselow and R. Howe, *Springer Tracts in Chemical Physics*, Vol. 35 (Springer, Berlin, 1984), p. 231.

<sup>14</sup>For O-O backscattering one obtains  $R_2^{901} = 3.37(8) \text{ \AA}$  and for O-Ni  $3.48(8) \text{ \AA}$ .

<sup>15</sup>R. W. Godby and N. Garcia, *Surf. Sci.* **163**, L681 (1985).

<sup>16</sup>S. Mukherjee, V. Kumar, and K. H. Bennemann (unpublished).

<sup>17</sup>H. Niehus (private communication).

<sup>18</sup>R. J. Behm, G. Ertl, V. Penka, and R. Schwanker, *J. Vac. Sci. Technol. A* **3**, 1595 (1985).

<sup>19</sup>R. Feidenhans'l and I. Steensgard, *Surf. Sci.* **133**, 453 (1983).

<sup>20</sup>J. Lapujoulade, Y. Le Cruër, M. Lefort, Y. Lejay, and E. Maurel, *Surf. Sci.* **118**, 103 (1982).